LISA: Modeling Tilt-to-length and Hermite-Gauss Modes in Python

Paul Edwards
University of Florida

A Python module, PauLisa.py, was developed and used to calculate Hermite-Gauss(HG) modes. Beam tilts and misalignments relative to the optical axis can be used to model tilt-to-length(TTL) coupling in LISA. This document presents theory and results of these calculations produced in the Jupyter Notebook IDE. Output of PauLisa.py shows good agreement with theory.

Contents

1 Hermite-Gauss Modes

Hermite-Gauss (HG) modes represent a set of exact solutions of the paraxial wave equation

$$\nabla_t^2 u(x,y,z) - 2ik\partial z u(x,y,z) = 0\,. \tag{1}$$

The Living Reviews article [1] gives the general expression for HG modes as

$$u_{nm}(x,y,z) = (2^{n+m-1}n!m!\pi)^{-1/2}\frac{1}{w(z)}H_n\Big(\frac{\sqrt{2}x}{w(z)}\Big)H_m\Big(\frac{\sqrt{2}y}{w(z)}\Big)\exp\Big(\frac{-ik(x^2+y^2)}{2R_c(z)} - \frac{x^2+y^2}{w(z)^2}\Big)\,. \tag{2}$$

In terms of the Gaussian beam parameter,

$$q(z) = iz_R + z - z_0 = q_0 + z - z_0\,, \tag{3}$$

HG modes may be expressed as (where $w(z) = w_0\sqrt{1+\left(\frac{z-z_0}{z_R}\right)^2}$):

$$\begin{aligned} u_{nm}(x,y,z) =& u_n(x,z)u_m(y,z) \\ =& \Big(\frac{2}{\pi}\Big)^{1/4}\Big(\frac{1}{2^n n! w_0}\Big)^{1/2}\Big(\frac{q_0}{q(z)}\Big)^{1/2}\Big(\frac{q_0 q*(z)}{q_0 * q(z)}\Big)^{n/2}H_n\Big(\frac{\sqrt{2}x}{w(z)}\Big)\exp\Big(\frac{-ik(x^2)}{2q_z}\Big)\times u_m(y,z)\,, \end{aligned} \tag{4}$$

where the first three Hermite polynomials are given by

$$H_n(x) = \begin{cases} 1 & (n=0) \\ 2x & (n=1) \\ 4x^2-2 & (n=2) \end{cases}$$

The HG modes are orthonormal, such that

$$\int\int dxdy\; u_{nm}u^*_{n'm'} = \delta_{nn'}\delta_{mm'}. \tag{5}$$

For approximations used in later sections, it is useful to express higher-order modes in terms of the fundamental mode. For $n = 0, 1, 2$ and $m = 0$ at the beam waist(letting $z_0 = 0$):

$$u_{00}(x,y,0) = \Big(\frac{2}{\pi}\Big)^{1/2}\Big(\frac{1}{w_0}\Big)\exp\left[-\Big(\frac{x^2+y2}{w_0^2}\Big)\right]\,, \tag{6}$$

$$u_{10}(x,y,0) = \Big(\frac{2}{\pi}\Big)^{1/2}\Big(\frac{2x}{w_0^2}\Big)\exp\left[-\Big(\frac{x^2+y2}{w_0^2}\Big)\right]\,, \tag{7}$$

$$u_{20}(x,y,0) = \Big(\frac{2}{\pi}\Big)^{1/2}\left[\Big(\frac{2\sqrt{2}x^2}{w_0^3}\Big) - \frac{\sqrt{2}}{2}\right]\exp\left[-\Big(\frac{x^2+y2}{w_0^2}\Big)\right]\,, \tag{8}$$

Expressing u_{10} and u_{20} in terms of u_{00} at the beam waist,

$$u_{10}(x,y,0) = \frac{2x}{w_0}u_{00}(x,y,0) \tag{9}$$

$$u_{20}(x,y,0) = \left[2\sqrt{2}\left(\frac{x^2}{w_0^2}\right) - \frac{\sqrt{2}}{2}\right] u_{00}(x,y,0) \tag{10}$$

In PauLisa.py, Eq. 2 is represented by the *calculate* function and Eq. 4 as *calculate_q*. The outputs of both functions agree exactly. In the appendix, intensity profiles produced by PauLisa.py for u_{00} to u_{33} are shown in Fig. A.1.

2 Shifted Beam Approximation

For a small shift of the input axis, $a<<w_0$, in the +x-direction relative to the cavity axis, the shifted u_{00} mode can be solved in terms of an added u_{10} mode up to a constant factor.

2.1. Shifted Beam : $z = z_0$

At $z = z_0 = 0$, a shifted beam can be expresssed as

$$\begin{aligned}
u_{00}(x-a,y,0) =& \Big(\frac{2}{\pi}\Big)^{-1/2}\Big(\frac{1}{w_0}\Big)\exp\Big(-\frac{(x-a)^2+y^2}{w_0^2}\Big)\\
=& \Big(\frac{2}{\pi}\Big)^{-1/2}\Big(\frac{1}{w_0}\Big)\exp\Big(-\frac{y^2}{w_0^2}\Big)\exp\Big(-\frac{(x-a)^2}{w_0^2}\Big)\\
=& u_{00}(x,y,0)\times exp\Big(\frac{2ax+a^2}{w_0^2}\Big)\\
=& u_{00}(x,y,0)\left[1+\frac{2ax}{w_0^2}+\mathcal{O}\Big(\frac{a}{w}\Big)^2\right]\\
\approx& u_{00}+\Big(\frac{2ax}{w_0^2}\Big)u_{00}\\
=& u_{00}(x,y,0)+\frac{a}{w_0}u_{10}(x,y,0)\ .
\end{aligned} \tag{11}$$

The phase is 0, as expected from the Gouy phase. The shift for mode coefficients C_{nm} is then

$$a \approx \frac{\Re(C_{10})}{\Re(C_{00})}w_0\ . \tag{12}$$

Results for HG(0,0) and HG(1,0) addition are shown in Fig. 2.

(1,0) Scale	Pred. Shift[$\times 10^{-5}m$]	Act. Shift[$\times 10^{-5}m$]	%Error
0.04	4.0	3.9849	0.37
0.08	8.0	7.8998	1.25
0.16	16.0	15.2546	4.65

TABLE (I) Calculated and predicted shift in peaks for varying scales of HG_{10} added in phase to HG_{00}.

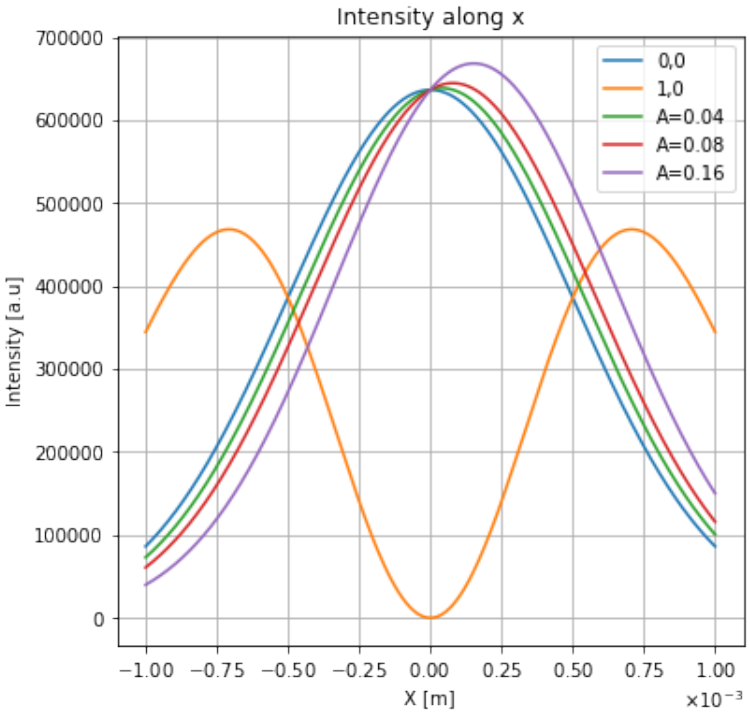

FIG. (2) Intensity at the beam waist and $y = 0$ for HG(0,0) and HG(1,0) modes alongside combined modes. The variable A represents the scale of the HG(1,0) mode, where 1 is the HG(0,0) mode coefficient.

2.2. Shifted Beam : $z = z_R$

At $z = z_R$, U_{10} ITO U_{00} is

$$U_{10}(x, y, z_R) = U_{00}(x, y, z_R) \left[1 + \frac{\sqrt{2}x}{w_0}\right] \tag{13}$$

For a shifted beam with $(z = z_R)$:

$$\begin{aligned} u_{tilt(0,0)}(x, y, z = z_R) =& u_{00} \exp\left[ik\Big(\frac{2ax}{4z_R}\Big)\right] \exp\left[\frac{ax}{w_0^2}\right] \\ \approx& u_{00}\left[1 + ik\Big(\frac{ax}{2z_R}\Big) + \frac{\sqrt{2}ax}{w_0^2}\right] \\ =& u_{00}(x, y, 0) + \left[i\frac{1}{\sqrt{2}} + \frac{1}{\sqrt{2}}\right]\Big(\frac{a}{w_0}\Big)u_{10}(x, y, 0)\ . \end{aligned} \tag{14}$$

The phase is $\frac{\pi}{4}$, in agreement with the Guoy phase.

2.3. Shifted Beam : $z >> z_R$

At $z >> z_R$, U_{10} ITO U_{00} is

$$U_{10}(x, y, z >> z_R) = \Big(\frac{2xz_R}{zw_0}\Big)U_{00}(x, y, z >> z_R) \tag{15}$$

Then, for a tilted beam with $(z >> z_R)$:

$$\begin{aligned} u_{tilt(0,0)}(x, y, z >> z_R) =& u_{00} \exp\left[ik\Big(\frac{ax}{z}\Big)\right] \exp\left[\frac{2ax}{w_0^2}\Big(\frac{z_R}{z}\Big)^2\right] \\ \approx& u_{00}\left[1 + ik\Big(\frac{ax}{z}\Big)\right]\left[1 + \frac{2ax}{w_0^2}\Big(\frac{z_R}{z}\Big)^2\right] \\ =& u_{00}(x, y, z >> z_R) + \left[\frac{z_R}{z} + i\right]\Big(\frac{a}{w_0}\Big)u_{10}(x, y, z >> z_R)\ . \end{aligned} \tag{16}$$

The phase is $\frac{\pi}{2}$, in agreement with the Guoy phase.

3 Tilted Beam Approximation

The following subsections show that a tilted beam at varying propagation distances can also be approximated as a sum of U_{00} and U_{10} modes, with an imaginary component in theU_{10} contribution.

3.1. Tilted Beam : $z = z_0$

For a tilt with added phase in x:

$$u_{tilt}(x, y, 0) = u_{00}(x, y, 0) \exp(i\phi)\ . \tag{17}$$

This phase is a result of transforming $x \to x\cos\alpha$ and $z \to z - xsin\alpha$.

Approximating this in terms of a quadrature phase addition of u_{10}, with $\alpha << \frac{\lambda}{w_0 \pi}$:

$$\begin{aligned} u_{tilt(0,0)} =& u_{00} \exp(i\phi) \\ =& u_{00} \exp\left[ikx \sin(\alpha)\right] \\ \approx& u_{00} \exp\left[ikx\alpha\right] \\ =& u_{00} \exp\left[i\left(\frac{2\pi x\alpha}{\lambda}\right)\right] \\ \approx& u_{00}\left[1 + i\left(\frac{2\pi x\alpha}{\lambda}\right)\right] \\ =& u_{00}(x, y, 0) + i\left(\frac{\pi w_0 \alpha}{\lambda}\right) u_{10} \ . \end{aligned} \tag{18}$$

Therefore, the predicted angle scales proportionally with the coefficient of the u_{10} mode, C_{10},

$$\alpha \approx \frac{|\Im(C_{10})|}{\Re(C_{00})} \frac{\lambda}{\pi w_0} \approx \frac{|\Im(C_{10})|}{\Re(C_{00})} \Theta \ , \tag{19}$$

where $\Theta = \frac{\pi w_0}{\lambda}$ is the diffraction angle. Results for HG_{10} quadrature-phase addition are shown in Table 2. Graphical results are shown in Fig. 3.

(1,0) Scale (Imag.)	Pred. Angle[$\times 10^{-5}$ rad.]	Act. Angle[$\times 10^{-5}$ rad.]	%Error
0.04	1.3547	1.3518	0.00212
0.08	2.7094	2.6866	0.00840
0.16	5.4189	5.2445	0.03217

TABLE (II) Calculated and expected wavefront angles for varying scales of HG_{10} added in quadrature phase to HG_{00}.

By Eq. 18, phase should vary with x as

$$\frac{d\phi}{dx} \approx \frac{2\pi\alpha}{\lambda} \ . \tag{20}$$

Figure 4 shows agreement with this approximation.

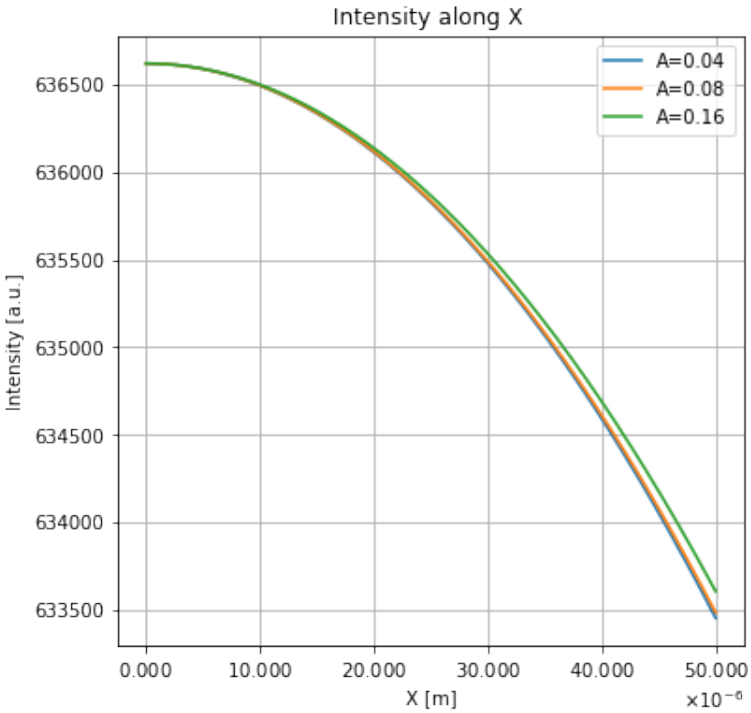

FIG. (3) Intensity at the beam waist and $y = 0$ for HG(0,0) and HG(1,0) addition in quadrature phase. The variable A represents the (imaginary) scale of the HG(1,0) mode, where 1 is the HG(0,0) mode coefficient.

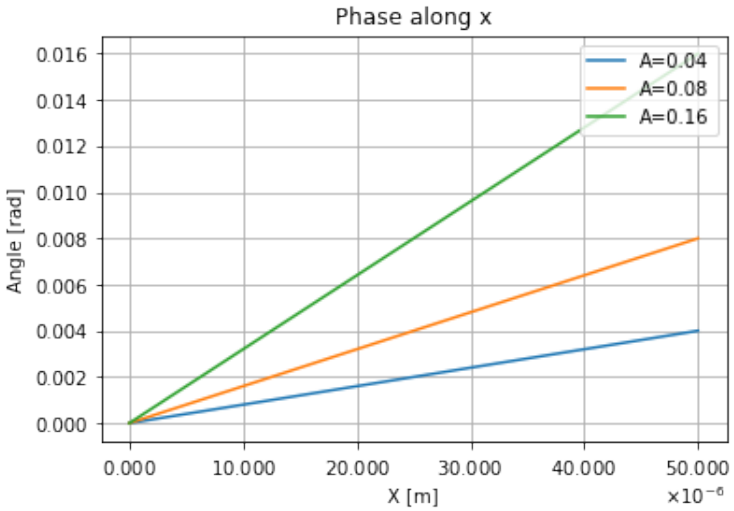

FIG. (4) Phase at the beam waist and $y = 0$ for HG(0,0) and HG(1,0) modes alongside combined modes. The variable A represents the (imaginary) scale of the HG(1,0) mode, where 1 is the HG(0,0) mode coefficient. Phase varies with x as predicted by Eq. 20

4 Tilting a Misaligned Beam

Building on the two previous sections, a tilt to an already shifted beam is

$$\sum_{n,m} u_{nm}(x,y,0) = u_{00(tilt)}(x,y,0) + \Big(\frac{a}{w_0}\Big) u_{10(tilt)}(x,y,0)\ . \tag{21}$$

Following the same approximations for a general tilted beam ($\alpha << \frac{\lambda}{w_0 \pi}$), the first term is the same as in Eq. 18,

$$u_{00(tilt)}(x,y,0) = u_{00}(x,y,0) + i\Big(\frac{\pi w_0 \alpha}{\lambda}\Big) u_{10}\ ,$$

while the u_{10} term in Eq. 21 is:

$$\begin{aligned}
\Big(\frac{a}{w_0}\Big) u_{10(tilt))}(x,y,0) =& \Big(\frac{a}{w_0}\Big) u_{10} \exp(i\phi) \\
=& \Big(\frac{a}{w_0}\Big) u_{10} \exp\left[ikx \sin(\alpha)\right] \\
\approx& \Big(\frac{a}{w_0}\Big) u_{10} \exp\left[ikx\alpha\right] \\
=& \Big(\frac{a}{w_0}\Big) u_{10} \exp\left[i\Big(\frac{2\pi x \alpha}{\lambda}\Big)\right] \\
\approx& \Big(\frac{a}{w_0}\Big) u_{10} \left[1 + i\Big(\frac{2\pi x \alpha}{\lambda}\Big)\right]\ .
\end{aligned} \tag{22}$$

In terms of u_{00}, the imaginary term in Eq. 22 is:

$$i\Big(\frac{2\pi x \alpha}{\lambda}\Big) u_{10} = i\Big(\frac{4\pi x^2 \alpha a}{w_0^2 \lambda}\Big) u_{00}\ . \tag{23}$$

Rewriting in terms of u_{00} and u_{20}:

$$i\Big(\frac{4\pi x^2 a \alpha}{w_0^2 \lambda}\Big) u_{00} = i\Big(\frac{2\pi \alpha a}{\sqrt{2}\lambda}\Big) \left[u_{20} + \frac{\sqrt{2}}{2} u_{00}\right]\ . \tag{24}$$

Therefore, Eq. 21 for a shifted then tilted beam of fundamental mode at the waist is

$$\sum_{n,m} u_{nm}(x,y,0) = \left[1 + i\Big(\frac{\pi a \alpha}{\lambda}\Big)\right] u_{00} + \left[\frac{a}{w_0} + i\Big(\frac{\pi w_0 \alpha}{\lambda}\Big)\right] u_{10} + i\Big(\frac{\sqrt{2}\pi a \alpha}{\lambda}\Big) u_{20}\ . \tag{25}$$

5 Tilt-to-Length Coupling

LISA uses PD's to measure interference of a received beam with a reference beam, resulting in beat notes which are used to determine phase difference ($\Delta\phi = \phi_1 - \phi_2$) of the two beams. Fields of the reference and received beam defined with a basis (w_0, z_0) are, respectively:

$$E_{ref} = E_{0\ (ref)} e^{i((\omega_{ref} t)+\phi_1)} u_{00}(w_{0\ ref}, z_{0\ ref})\ . \tag{26}$$

$$E_{rec} = E_{0\ (rec)} e^{i((\omega_{rec} t)+\phi_2)} \sum_{n,m=0} u_{nm}(w_{0\ rec}, z_{0\ rec})\ , \tag{27}$$

These fields produce a power at a single PD (assuming the PD area is large relative to the beam)

$$P_{pd} = \int_{-\infty}^{\infty}\int_{-\infty}^{\infty} E^* E\ dxdy, \tag{28}$$

where the electric field is the sum of the received and reference fields. Let the spatial component of the received beam be given by Eq. 25. By orthonormality of HG modes, only the imaginary part of the received beam's u_{00} mode contributes to an overall phase shift. The sum of the electric fields of the received and reference beam of the same basis is, effectively,

$$E = E_{0(ref)} e^{i((\omega_{ref} t)+\phi_1)} u_{00} + E_{0(rec)} e^{i((\omega_{rec} t)+\phi_2)} u_{00} \left[1 + i\Big(\frac{\pi a \alpha}{\lambda}\Big)\right]\ , \tag{29}$$

and, condensing the E_0 terms,

$$E^* E = u_{00}^* u_{00} |E_0|^2 \{2 + (\frac{\pi a \alpha}{\lambda})^2 + e^{i(\Delta\omega t+\Delta\phi)}\left[1 - i\frac{\pi a \alpha}{\lambda}\right] + e^{-i(\Delta\omega t+\Delta\phi)}\left[1 + i\frac{\pi a \alpha}{\lambda}\right]\}\ . \tag{30}$$

Neglecting time-independent terms and u_{00} (factors by orthornormality), and letting $\Delta\omega = \omega_{0ref} - \omega_{0rec}$:

$$\begin{aligned} E^* E =& |E_0|^2 \{e^{i(\Delta\omega t+\Delta\phi)}\left[1 - i\frac{\pi a \alpha}{\lambda}\right] + e^{-i(\Delta\omega t+\Delta\phi)}\left[1 + i\frac{\pi a \alpha}{\lambda}\right]\} \\ =& |E_0|^2 \{\left[e^{i(\Delta\omega t+\Delta\phi)} + e^{-i(\Delta\omega t+\Delta\phi)}\right] + i\frac{\pi a \alpha}{\lambda}\left[e^{-i(\Delta\omega t+\Delta\phi)} - e^{i(\Delta\omega t+\Delta\phi)}\right]\} \\ =& 2|E_0|^2 \{\cos(\Delta\omega t + \Delta\phi) + \frac{\pi a \alpha}{\lambda}\sin(\Delta\omega t + \Delta\phi)\}\ . \end{aligned} \tag{31}$$

On demodulating and neglecting $\Delta\phi$ at the phasemeter, the I signal is

$$\begin{aligned} I =& E^* E \times \cos(\Delta\omega t) \\ =& 2|E_0|^2 \{\cos(\Delta\omega t) + \frac{\pi a \alpha}{\lambda}\sin(\Delta\omega t)\} \times \cos(\Delta\omega t) \\ =& |E_0|^2 \{1 + \cos(2\Delta\omega t) + \frac{\pi a \alpha}{\lambda}\sin(2\Delta\omega t)\}\ , \end{aligned} \tag{32}$$

and the Q signal is

$$\begin{aligned} Q =& E^* E \times \sin(\Delta\omega t) \\ =& 2|E_0|^2 \{\cos(\Delta\omega t) + \frac{\pi a \alpha}{\lambda}\sin(\Delta\omega t)\} \times \sin(\Delta\omega t) \\ =& |E_0|^2 \{\frac{\pi a \alpha}{\lambda}(1 - \cos(2\Delta\omega t)) + \sin(2\Delta\omega t)\}\ , \end{aligned} \tag{33}$$

Therefore, after a low pass filter (as the heterodyne frequency is on the order of MHz), the phase is linear in shift and tilt

$$\begin{aligned}\Phi &= \arctan(\frac{Q}{I}) \\ &= \arctan\left(\frac{\frac{\pi a \alpha}{\lambda}}{1}\right) \\ &\approx \frac{\pi a \alpha}{\lambda} \ .\end{aligned} \tag{34}$$

Shifting a misaligned beam would have rendered the same approximation. Compared to a single misalignment of a beam (Eq. 18), which only has a phase shift contribution via a u_{10} term, the shifted and tilted beam has phase shift via a u_{00} term in quadrature phase to the reference beam. Moreover, the S/C rotating about the CoM of the TM means the beam with a waist centered on the TM also appears to rotate about the TM CoM, resulting in no TTL coupling as the wavefronts at the receiving S/C appear spherically centered on the TM CoM. The result of a misaligned then tilted beam, however, is tilt-to-length coupling, where jitter has coupled into length.

Section C of the LISA Payload Description Document (PDD) outlines expected TTL couplings and tolerances:

- **S/C jitter** $\sim 10\ \text{nrad}/\sqrt{\text{Hz}}$
- **OB Lateral alignment offset** $\sim 20\ \mu m$
- **Combined** $\sim 20\ \text{pm}/\sqrt{\text{Hz}}$

6 Modulating TTL over LISA's Long Arm

Jitter of a tilted beam, as outlined in the previous section, can be used to model TTL coupling in LISA's long arm. Sinusoidal modulation of the terms in Eq. 25 which came as an effect of jitter, scaled in m, yields:

$$u(x,y,0) = \left[u_{00} + \frac{a}{w_0}u_{10}\right] + i\frac{\pi\alpha}{\lambda}\left[a\Big(u_{00} + \sqrt{2}u_{20}\Big) + w_0 u_{10}\right] m\sin(\omega t - \phi)\ . \tag{35}$$

Assume an arm of 2.5 Gm, $w_0 = 15$ cm, and PD radius = 15 cm.

7 Movable Aperture

The MA in Fig. 5 is designed to reduce TTL coupling via adjustable compensation during mission maintenance sessions. A discrete, artificial jitter applied to the S/C generates a measurable offset which may be subtracted with positional calibration of the MA.

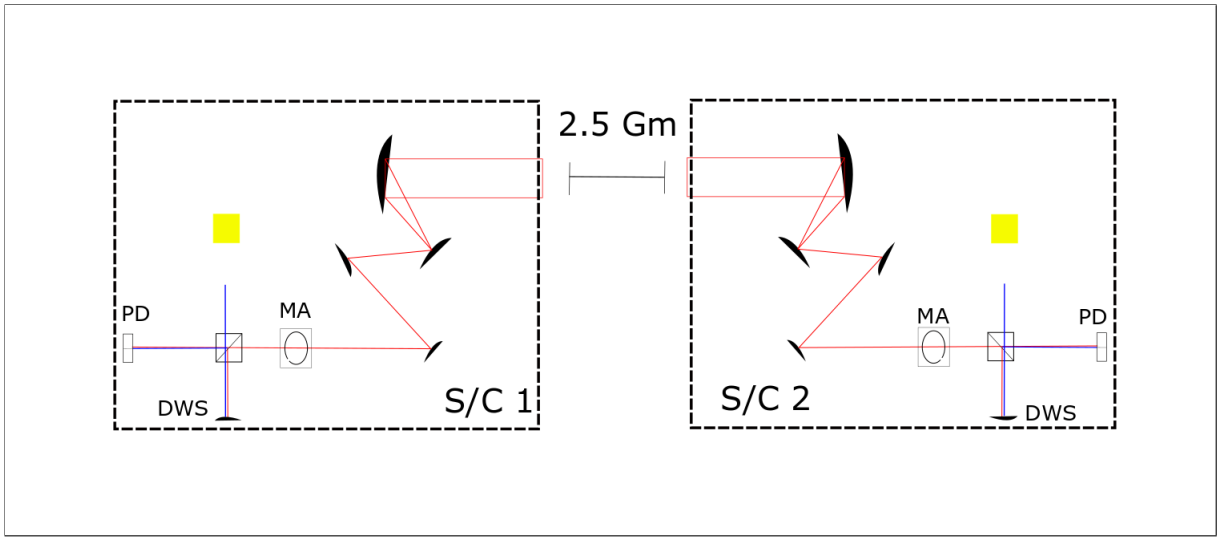

FIG. (5) Incoming beam (red) passes a movable aperture and interferes with local beam (blue).

8 Tilted Beam at Half-Plane

8.1. Gapless Approximation

Initially, we describe a tilted beam, incoming from S/C 1, interfering with a Gaussian local beam at S/C 2. The incoming tilted beam ITO HG modes is

$$U_{RX}(x,y,z) = U_{00}(x,y,z) + i\Big(\frac{\pi w_0 \alpha}{\lambda}\Big)U_{10}(x,y,z)\ .$$

Using the planar HG representation:

$$u_{nm}(x,y,z) = (2^{n+m-1}n!m!\pi)^{-1/2}\frac{1}{w(z)}H_n\Big(\frac{\sqrt{2}x}{w(z)}\Big)H_m\Big(\frac{\sqrt{2}y}{w(z)}\Big)\exp\Big(\frac{-ik(x^2+y^2)}{2R_c(z)} - \frac{x^2+y^2}{w(z)^2}\Big)\ .$$

with Hermite polynomials

$$H_n(x) = \begin{cases} 1 & (n=0) \\ 2x & (n=1) \end{cases}$$

For the PD right side:

$$\begin{aligned}
C^R_{nmn'm'} &= \int_0^\infty dx \int_{-\infty}^\infty dy\ U^*_{00(LO)}(x,y,z)U_{nm(RX)}(x,y,z) \\
&= \int_0^\infty dx \int_{-\infty}^\infty dy\ U^*_{00}\left[U_{00} + i\Big(\frac{\pi w_0\alpha}{\lambda}\Big)U_{10}\right] \\
&= \int_0^\infty dx \int_{-\infty}^\infty dy\ \left[\sqrt{\frac{2}{\pi}}\frac{1}{w(z)}\exp\Big(\frac{+ik\rho^2}{2R_c(z)} - \frac{\rho^2}{w(z)^2}\Big)\right]\times \\
&\quad \left[\sqrt{\frac{2}{\pi}}\frac{1}{w(z)}\exp\Big(\frac{-ik\rho^2}{2R_c(z)} - \frac{\rho^2}{w(z)^2}\Big) + i\Big(\frac{\pi w_0\alpha}{\lambda}\Big)\frac{1}{\sqrt{\pi}}\frac{1}{w(z)}2\Big(\frac{\sqrt{2}x}{w(z)}\Big)1\exp\Big(\frac{-ik\rho^2}{2R_c(z)} - \frac{\rho^2}{w(z)^2}\Big)\right] \\
&= \int_0^\infty dx \int_{-\infty}^\infty dy\ \left[\sqrt{\frac{2}{\pi}}\frac{1}{w(z)}\exp\Big(\frac{+ik\rho^2}{2R_c(z)} - \frac{\rho^2}{w(z)^2}\Big)\right]\times \\
&\quad \left[\sqrt{\frac{2}{\pi}}\frac{1}{w(z)}\exp\Big(\frac{-ik\rho^2}{2R_c(z)} - \frac{\rho^2}{w(z)^2}\Big) + i\Big(\frac{\sqrt{\pi}w_0\alpha}{\lambda}\Big)\Big(\frac{2\sqrt{2}x}{w(z)^2}\Big)\exp\Big(\frac{-ik\rho^2}{2R_c(z)} - \frac{\rho^2}{w(z)^2}\Big)\right] \\
&= \int_0^\infty dx \int_{-\infty}^\infty dy\ \left[\frac{2}{\pi}\frac{1}{w(z)^2}\exp\Big(\frac{-2\rho^2}{w(z)^2}\Big) + i\Big(\frac{w_0\alpha}{\lambda}\Big)\Big(\frac{4x}{w(z)^3}\Big)\exp\Big(\frac{-2\rho^2}{w(z)^2}\Big)\right]\ .
\end{aligned}$$

Finally,

$$C^R_{nmn'm'} = \int_0^\infty dx \int_{-\infty}^\infty dy\ \{\Big(\frac{2}{\pi w(z)^2}\Big)\exp\Big(\frac{-2\rho^2}{w(z)^2}\Big)\left[1 + i\Big(\frac{2\pi w_0\alpha x}{\lambda w(z)}\Big)\right]\}\ . \tag{36}$$

The real term ($a = \frac{2}{w(z)^2}$):

$$\begin{aligned}\Big(\frac{2}{\pi w(z)^2}\Big)\left[\int_0^\infty\int_{-\infty}^\infty e^{-ax^2}e^{-ay^2}dydx\right] =&\Big(\frac{2}{\pi w(z)^2}\Big)\frac{1}{2}(\sqrt{\frac{\pi}{a}})^2\\ =&\Big(\frac{2}{\pi w(z)^2}\Big)\frac{1}{2}\frac{w(z)^2\pi}{2}\\ =&\Big(\frac{2}{\pi w(z)^2}\Big)\frac{w(z)^2\pi}{4}\\ =&\frac{1}{2}\,.\end{aligned}$$

The imaginary term is ($a=\frac{2}{w(z)^2}$):

$$\begin{aligned}i\Big(\frac{4w_0\alpha}{\lambda w(z)^3}\Big)\left[\int_0^\infty\int_{-\infty}^\infty e^{-ax^2}xe^{-ay^2}dydx\right] =&i\Big(\frac{4w_0\alpha}{\lambda w(z)^3}\Big)\left[\sqrt{\frac{\pi}{a}}\int_0^\infty dx\; e^{-ax^2}x\right]\\ =&i\Big(\frac{4w_0\alpha}{\lambda w(z)^3}\Big)\left[\sqrt{\frac{\pi}{a}}\frac{1}{2a}\right]\\ =&i\Big(\frac{w_0\alpha}{\lambda w(z)}\Big)\left[\sqrt{\frac{\pi w(z)^2}{2}}\right]\\ =&i\sqrt{\frac{\pi}{2}}\frac{w_0\alpha}{\lambda}\,.\end{aligned}$$

So the right side is

$$C^R_{nmn'm'}=\frac{1}{2}+i\sqrt{\frac{\pi}{2}}\frac{w_0\alpha}{\lambda}\,, \tag{37}$$

and the left side is (as $\int_{-\infty}^0 dx\; xe^{-ax^2}=-\frac{1}{2a}$)

$$C^L_{nmn'm'}=\frac{1}{2}-i\sqrt{\frac{\pi}{2}}\frac{w_0\alpha}{\lambda}\,. \tag{38}$$

The phase of the right side:

$$\begin{aligned}\phi_R =&arg\left[\sum_n\sum_m A_{nm}C^R_{nm00}\right]\\ =&arg\left[\frac{1}{2}+i\sqrt{\frac{\pi}{2}}\frac{w_0\alpha}{\lambda}\right]\\ =&\arctan\Big(\frac{\sqrt{2\pi}w_0\alpha}{\lambda}\Big)\,.\end{aligned}$$

The phase of the left side:

$$\begin{aligned}\phi_L =&arg\left[\sum_n\sum_m A_{nm}C^L_{nm00}\right]\\ =&arg\left[\frac{1}{2}-i\sqrt{\frac{\pi}{2}}\frac{w_0\alpha}{\lambda}\right]\\ =&\arctan\Big(\frac{-\sqrt{2\pi}w_0\alpha}{\lambda}\Big)\\ =&-\phi_R\,.\end{aligned}$$

The offset:

$$\begin{aligned}\Delta\phi &= \frac{1}{2}\left[\phi_R - \phi_L\right] \\ &= \phi_R \ .\end{aligned}$$

Therefore, the solution is (plotted in Fig. 6):

$$\Delta\phi(\alpha) = \arctan(\frac{\sqrt{2\pi}w_0\alpha}{\lambda}). \tag{39}$$

Taking the derivative WRT α (shown in Fig. 7):

$$\frac{d\Delta\phi}{d\alpha} = \frac{1}{1+(\frac{\sqrt{2\pi}w_0\alpha}{\lambda})^2}\frac{\sqrt{2\pi}w_0}{\lambda} \tag{40}$$

$$= \frac{\sqrt{2\pi}w_0\lambda}{\lambda^2 + 2\pi w_0^2\alpha^2}. \tag{41}$$

Alex's result (shown in Fig. 8, with derivative in Fig. 9):

$$\Phi_{dif} = \arctan\left[\mathrm{erfi}(\frac{kw(z)\sin\alpha}{2\sqrt{2}})\right] \tag{42}$$

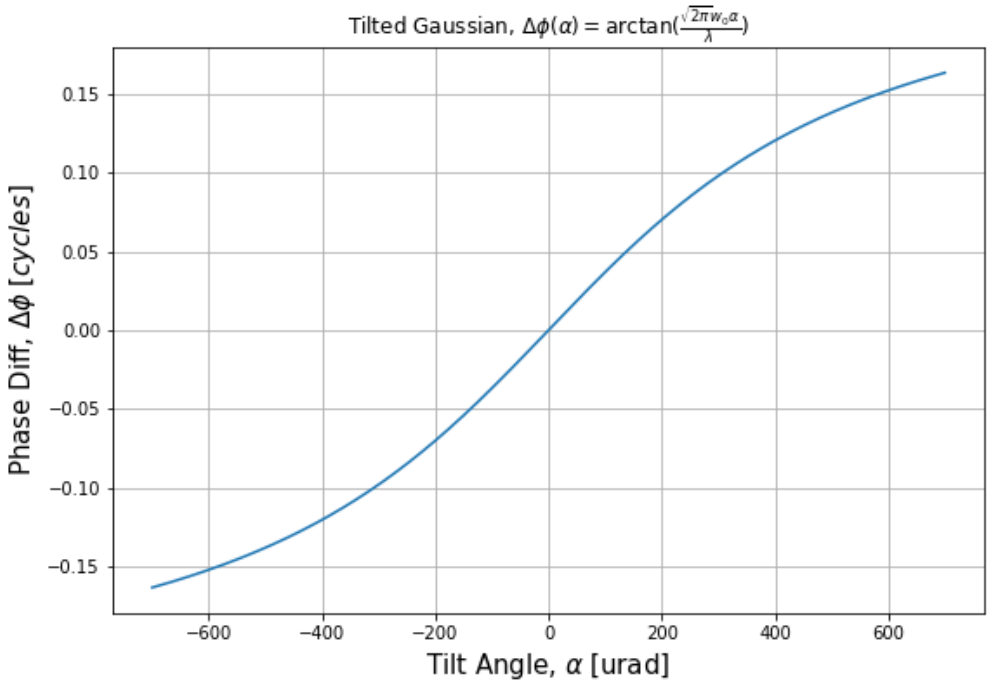

FIG. (6) Initial result.

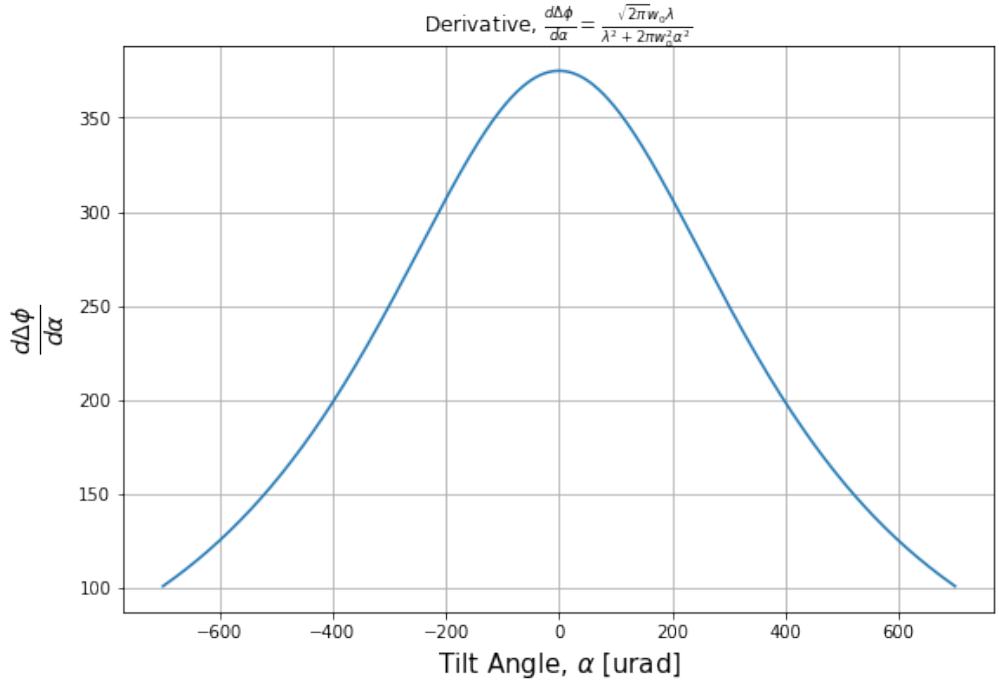

FIG. (7) Der. initial result tilted beam.

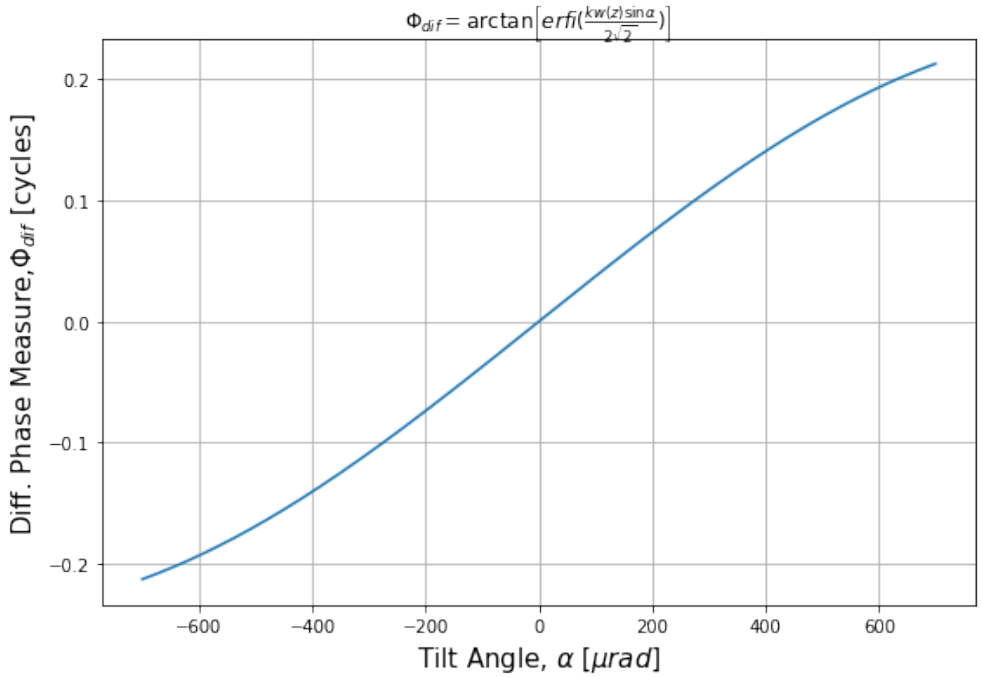

FIG. (8) Alex work.

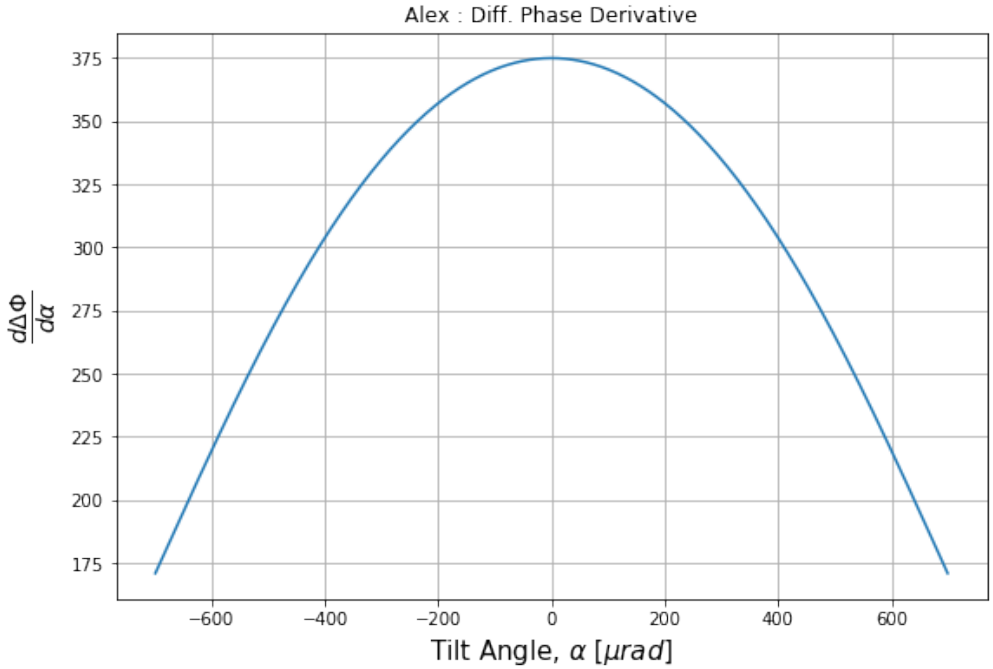

FIG. (9) Der. Alex work tilted beam.

8.2. Length Calculation by Demodulation Formalism

As in Sn. 5, power at the right PD is

$$P_{pd,R} = \int_{-\infty}^{\infty}\int_{0}^{\infty} E^* E dx dy,$$

and the left is

$$P_{pd,L} = \int_{-\infty}^{\infty}\int_{-\infty}^{0} E^* E dx dy,$$

The field is (suppressing amplitude E_0):

$$E = e^{i(w_1 t+\phi_1)}u_{00} + e^{i(\omega_2 t+\phi_2)}\left[u_{00} + i\Big(\frac{\pi w_0 \alpha}{\lambda}\Big)u_{10}\right], \tag{43}$$

simplifying then neglecting time-independent terms:

$$\begin{aligned}
E^*E =& u_{00}^* u_{00} + \left[u_{00}^* u_{00} + \Big(\frac{\pi\omega_0\alpha}{\lambda}\Big)^2 u_{10}^* u_{10} + i\Big(\frac{\pi\omega_0\alpha}{\lambda}\Big)u_{00}^* u_{10} - i\Big(\frac{\pi\omega_0\alpha}{\lambda}\Big)u_{10}^* u_{00}\right] \\
&+ u_{00}^*\left[u_{00} + i\Big(\frac{\pi w_0\alpha}{\lambda}\Big)u_{10}\right]e^{-i(\Delta\omega t+\Delta\phi)} + \left[u_{00}^* - i\Big(\frac{\pi w_0\alpha}{\lambda}\Big)u_{10}^*\right]u_{00}e^{i(\Delta\omega t+\Delta\phi)} \\
=& \left[\|u_{00}\|^2 + i\Big(\frac{\pi w_0\alpha}{\lambda}\Big)u_{00}^* u_{10}\right]e^{-i(\Delta\omega t+\Delta\phi)} + \left[\|u_{00}\|^2 - i\Big(\frac{\pi w_0\alpha}{\lambda}\Big)u_{00}u_{10}^*\right]e^{i(\Delta\omega t+\Delta\phi)}
\end{aligned}$$

The power at PD is then (using previous results):

$$\begin{aligned}
P_{pd} =& \left[\int_{-\infty}^{\infty}\int_{-\infty}^{0} E^*E\, dxdy\right] + \left[\int_{-\infty}^{\infty}\int_{0}^{\infty} E^*E\, dxdy\right] \\
=& \left[(\frac{1}{2} - i\sqrt{\frac{\pi}{2}}\frac{w_0\alpha}{\lambda})e^{-i(\Delta\omega t+\Delta\phi)} + (\frac{1}{2} + i\sqrt{\frac{\pi}{2}}\frac{w_0\alpha}{\lambda})e^{i(\Delta\omega t+\Delta\phi)}\right] \\
&+ \left[(\frac{1}{2} + i\sqrt{\frac{\pi}{2}}\frac{w_0\alpha}{\lambda})e^{-i(\Delta\omega t+\Delta\phi)} + (\frac{1}{2} - i\sqrt{\frac{\pi}{2}}\frac{w_0\alpha}{\lambda})e^{i(\Delta\omega t+\Delta\phi)}\right] \\
=& e^{-i(\Delta\omega t+\Delta\phi)} + e^{i(\Delta\omega t+\Delta\phi)} \\
=& 2\cos(\Delta\omega t + \Delta\phi)
\end{aligned}$$

Obviously, no TTL, and on I/Q demod, the in-phase:

$$\begin{aligned}
I =& 2\cos^2(\Delta\omega t) \\
=& 1 + \cos(2\Delta\omega t)
\end{aligned}$$

and quadrature:

$$\begin{aligned}
Q =& 2\cos(\Delta\omega t)\sin(\Delta\omega t) \\
=& \sin(2\Delta\omega t)
\end{aligned}$$

Thus, after a LPF, results agree with SN 8.1:

$$\Phi = \arctan\left(\frac{Q}{I}\right) = 0 \tag{44}$$

8.3. Gap Approximation

For a vertical(x-centered) gap of width $2b$ in the half-plane PD, the integrals in Sn. 7.1 become:

$$C^R_{nmn'm'} = \int_b^\infty dx \int_{-\infty}^\infty dy \, \{\Big(\frac{2}{\pi w(z)^2}\Big) \exp\Big(\frac{-2\rho^2}{w(z)^2}\Big) \Big[1 + i\Big(\frac{2\pi w_0 \alpha x}{\lambda w(z)}\Big)\Big]\} \, , \tag{45}$$

and

$$C^L_{nmn'm'} = \int_{-\infty}^{-b} dx \int_{-\infty}^\infty dy \, \{\Big(\frac{2}{\pi w(z)^2}\Big) \exp\Big(\frac{-2\rho^2}{w(z)^2}\Big) \Big[1 + i\Big(\frac{2\pi w_0 \alpha x}{\lambda w(z)}\Big)\Big]\} \, . \tag{46}$$

Integrating over the real term for the right side ($a = \frac{2}{w(z)^2}$):

$$\begin{aligned}\Big(\frac{2}{\pi w(z)^2}\Big)\Big[\int_b^\infty \int_{-\infty}^\infty e^{-ax^2} e^{-ay^2} dy dx\Big] =& \Big(\frac{2}{\pi w(z)^2}\Big)\Big[\frac{\sqrt{\pi}\,\mathrm{erfc}(\sqrt{a}b)}{2\sqrt{a}}\Big]\Big[\sqrt{\frac{\pi}{a}}\Big] \\ =& \frac{\mathrm{erfc}(\sqrt{a}b)}{w(z)^2 a} \\ =& \frac{1}{2}\mathrm{erfc}(\frac{\sqrt{2}b}{w(z)}) \, .\end{aligned}$$

The imaginary term is ($a = \frac{2}{w(z)^2}$):

$$\begin{aligned}i\Big(\frac{4w_0\alpha}{\lambda w(z)^3}\Big)\Big[\int_b^\infty \int_{-\infty}^\infty e^{-ax^2} x e^{-ay^2} dy dx\Big] =& i\Big(\frac{4w_0\alpha}{\lambda w(z)^3}\Big)\Big[\sqrt{\frac{\pi}{a}}\int_b^\infty dx\, e^{-ax^2} x\Big] \\ =& i\Big(\frac{4w_0\alpha}{\lambda w(z)^3}\Big)\Big[\sqrt{\frac{\pi}{a}}\frac{e^{-ab^2}}{2a}\Big] \\ =& i\frac{\sqrt{\pi} w_0 \alpha}{\sqrt{2}\lambda} e^{-\frac{2b^2}{w(z)^2}}\end{aligned}$$

So the right side is

$$C^R_{nmn'm'} = \frac{1}{2}\mathrm{erfc}(\frac{\sqrt{2}b}{w(z)}) + i\frac{\sqrt{\pi} w_0 \alpha}{\sqrt{2}\lambda} e^{-\frac{2b^2}{w(z)^2}} \, , \tag{47}$$

and the left is

$$C^L_{nmn'm'} = \frac{1}{2}\mathrm{erfc}(\frac{\sqrt{2}b}{w(z)}) - i\frac{\sqrt{\pi} w_0 \alpha}{\sqrt{2}\lambda} e^{-\frac{2b^2}{w(z)^2}} \, . \tag{48}$$

The phases are then (with plots in Fig. 10 and Fig. 11)

$$\begin{aligned}\phi_R =& -\phi_L = \Delta\phi \\ =& \arctan(\frac{\frac{\sqrt{\pi} w_0 \alpha}{\sqrt{2}\lambda} e^{-\frac{2b^2}{w(z)^2}}}{\frac{1}{2}\mathrm{erfc}(\frac{\sqrt{2}b}{w(z)})}) \\ =& \arctan\Big(\frac{\sqrt{2\pi} w_0 \alpha \, e^{-\frac{2b^2}{w(z)^2}}}{\lambda \, \mathrm{erfc}(\frac{\sqrt{2}b}{w(z)})}\Big)\end{aligned}$$

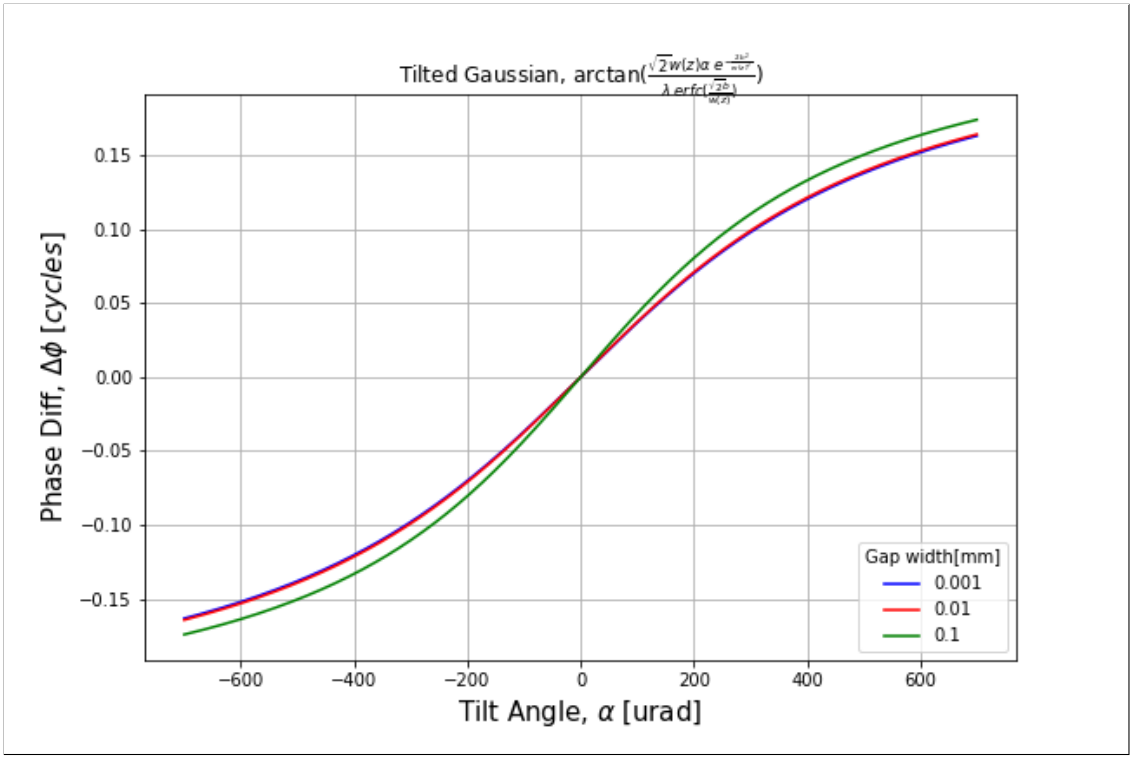

FIG. (10) Tilted beam at half-plane PD with centered, symmetric gap.

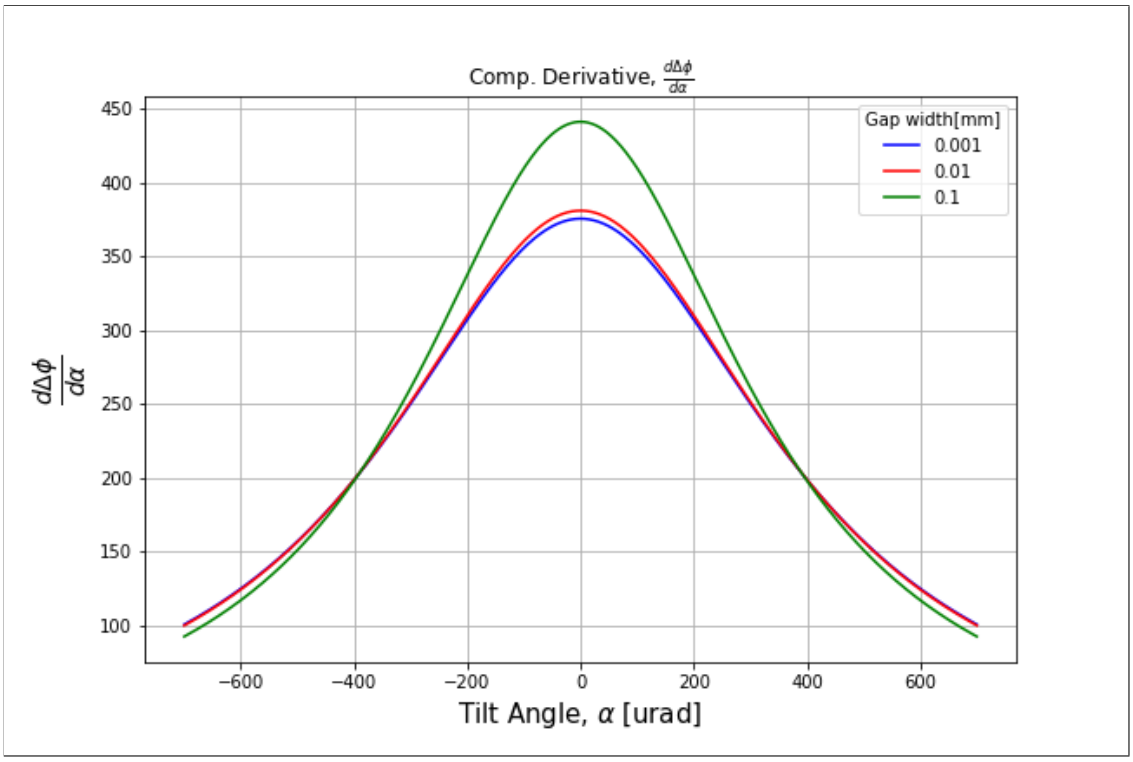

FIG. (11) Derivative for tilted beam at PD with centered, symmetric gap.

On setting the gap width to zero, the result of SN 8.1 (tilted beam approximation without gap) is recovered.
Alex also provided solutions (beyond immediate $e^{ikx\alpha} \approx 1 + ikx\alpha$ approximation).If the gap (of total width = d) is centered:

$$\Phi_{diff} = \arctan\left[\frac{erf(\frac{d}{\sqrt{2}w(z)} + \frac{ikw(z)\sin\alpha}{2\sqrt{2}}) - erf(\frac{d}{\sqrt{2}w(z)} - \frac{ikw(z)\sin\alpha}{2\sqrt{2}})}{i\Big(2 - erf(\frac{d}{\sqrt{2}w(z)} + \frac{ikw(z)\sin\alpha}{2\sqrt{2}}) - erf(\frac{d}{\sqrt{2}w(z)} - \frac{ikw(z)\sin\alpha}{2\sqrt{2}})\Big)}\right] \tag{49}$$

Results for the symmetric gap are shown in Fig. 12 and Fig. 13.
If, however, the gap is asymmetric (where s_l = distance at left and s_r = distance at right):

$$\begin{aligned}\Phi_{diff} = \frac{1}{2}\Bigg(&\arctan\left[\frac{erf(\frac{\sqrt{2}s_r}{w(z)} + \frac{ikw(z)\sin\alpha}{2\sqrt{2}}) - erf(\frac{\sqrt{2}s_r}{w(z)} - \frac{ikw(z)\sin\alpha}{2\sqrt{2}})}{i\Big(2 - erf(\frac{\sqrt{2}s_r}{w(z)} + \frac{ikw(z)\sin\alpha}{2\sqrt{2}}) - erf(\frac{\sqrt{2}s_r}{w(z)} - \frac{ikw(z)\sin\alpha}{2\sqrt{2}})\Big)}\right] \\ &+ \arctan\left[\frac{erf(\frac{\sqrt{2}s_l}{w(z)} + \frac{ikw(z)\sin\alpha}{2\sqrt{2}}) - erf(\frac{\sqrt{2}s_l}{w(z)} - \frac{ikw(z)\sin\alpha}{2\sqrt{2}})}{i\Big(2 - erf(\frac{\sqrt{2}s_l}{w(z)} + \frac{ikw(z)\sin\alpha}{2\sqrt{2}}) - erf(\frac{\sqrt{2}s_l}{w(z)} - \frac{ikw(z)\sin\alpha}{2\sqrt{2}})\Big)}\right]\Bigg)\end{aligned}$$

Results for the asymmetric gap are shown in Fig. 14 and Fig. 15.

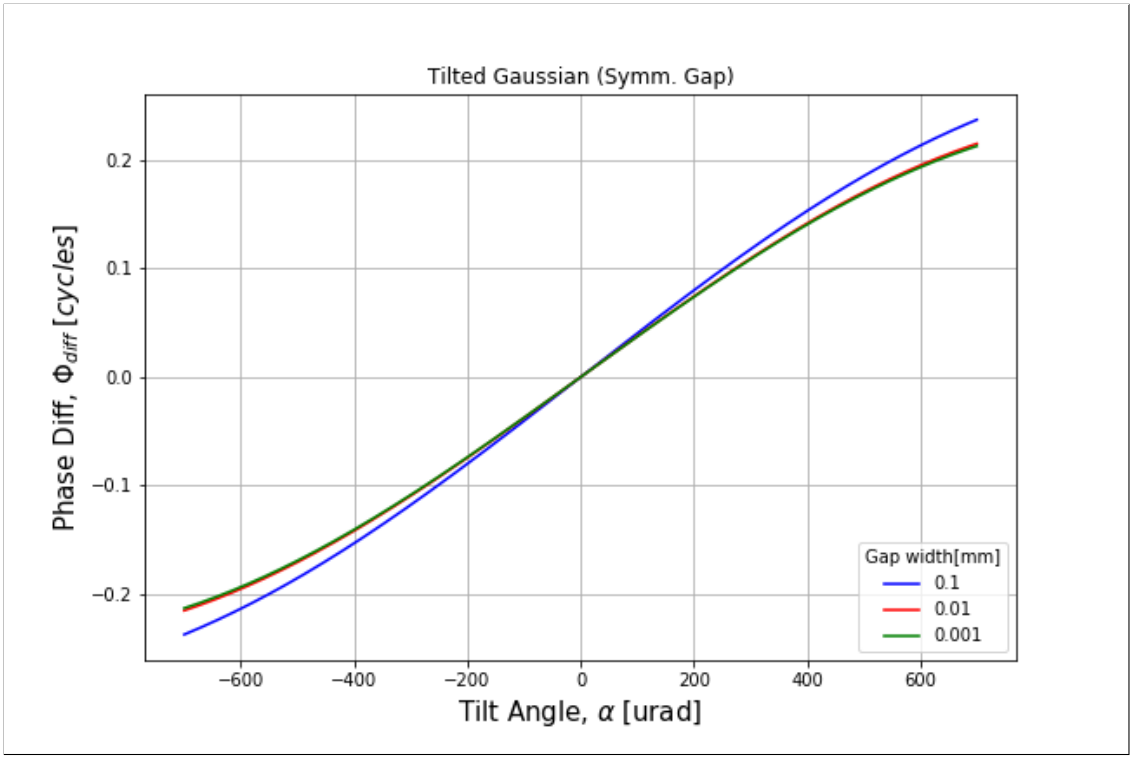

FIG. (12) AW result - Tilted beam at centered half-plane PD with gap.

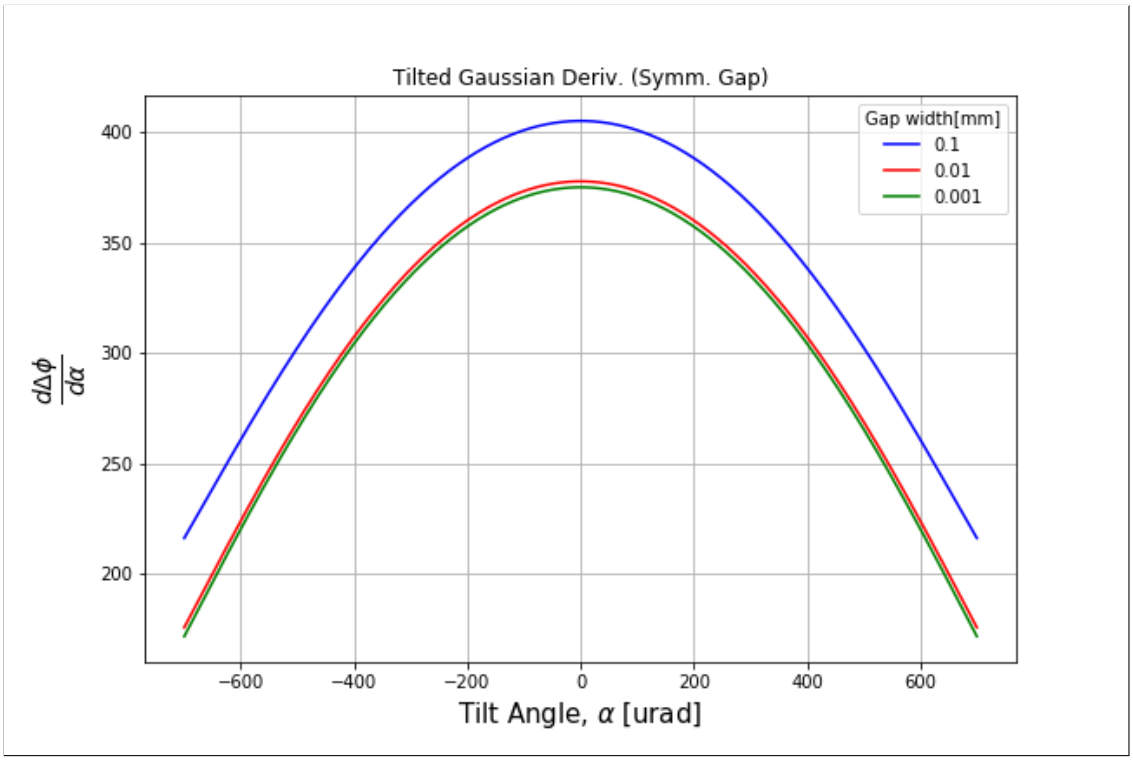

FIG. (13) AW result - Derivative for tilted beam at centered half-plane PD with gap.

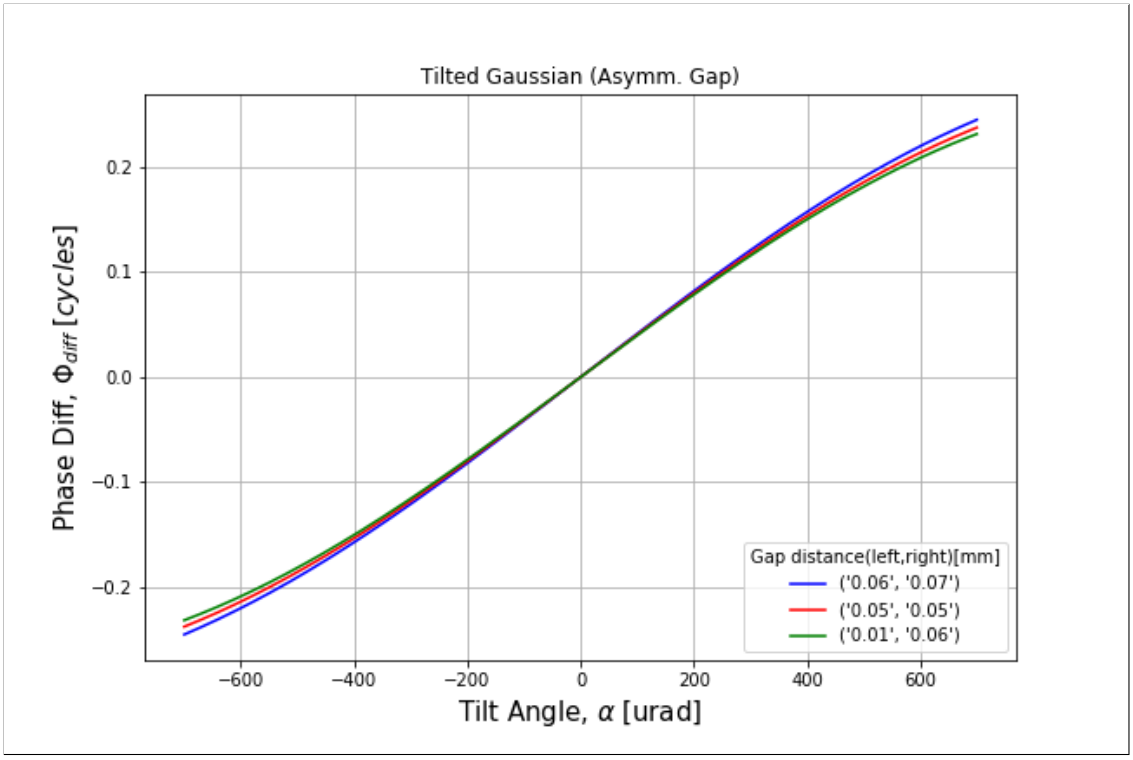

FIG. (14) AW result - Tilted beam at centered half-plane PD with asymmetric gap.

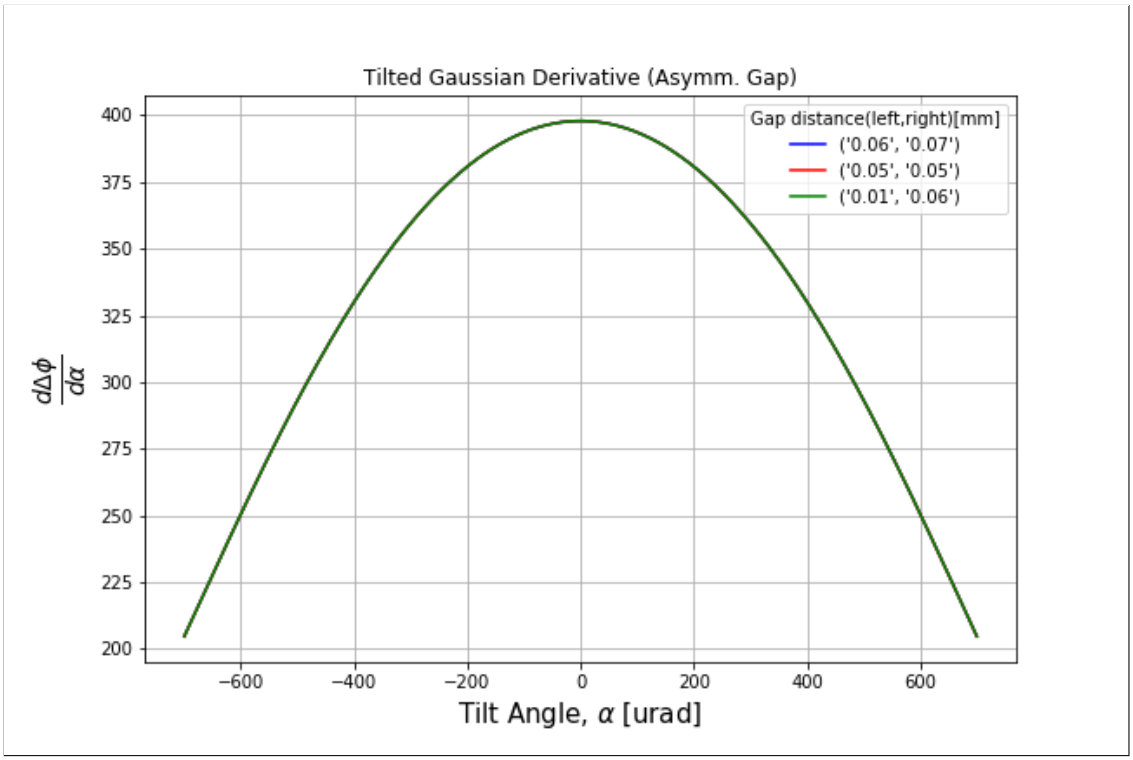

FIG. (15) AW result - Derivative for tilted beam at centered half-plane PD with asymmetric gap.

8.4. Tilted Beam Basis Mismatch

$$U_{nm}e^{ikx\alpha} = .$$

[1] C. Bond, D. Brown, A. Freise, and K. A. Strain, Living Reviews in Relativity **19**, 3 (2017), ISSN 1433-8351, URL https://doi.org/10.1007/s41114-016-0002-8.

A Intensity Plots

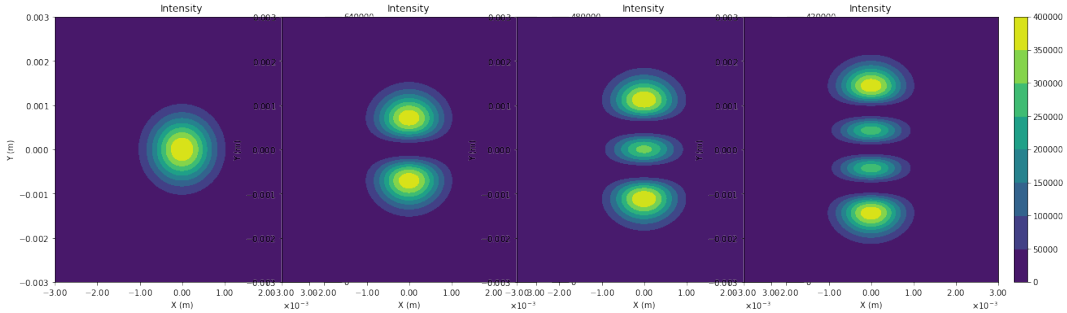

(a) HG(0,0) (b) HG(0,1) (c) HG(0,2) (d) HG(0,3)

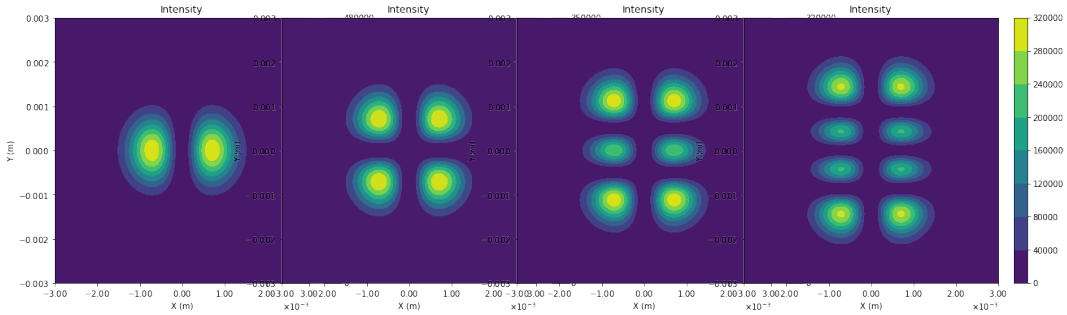

(e) HG(1,0) (f) HG(1,1) (g) HG(1,2) (h) HG(1,3)

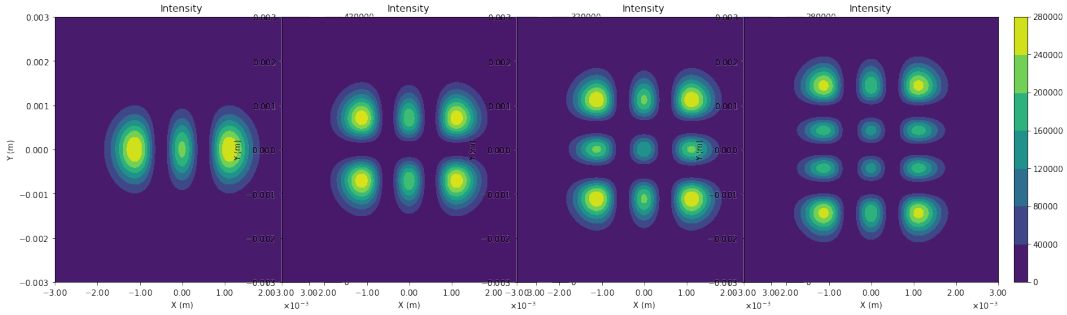

(i) HG(2,0) (j) HG(2,1) (k) HG(2,2) (l) HG(2,3)

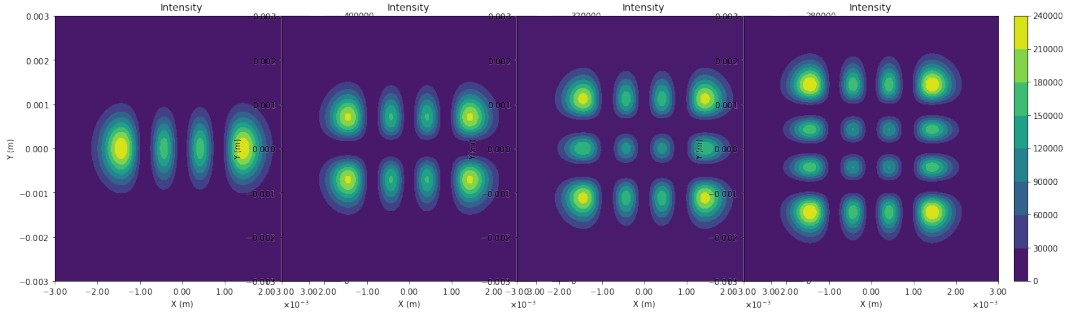

(m) HG(3,0) (n) HG(3,1) (o) HG(3,2) (p) HG(3,3)

FIG. (A.1) Intensity profiles for HG modes u_{00} to u_{33} at the beam waist.

B Acronyms

ACRONYMS

CoM	*center of mass*
HG	*Hermite – Gauss*
OB	*opticalbench*
PD	*photodetector*
PDD	*Payload Definition Document*
S/C	*spacecraft*
TM	*test mass*
TTL	*tilt to length*

C Optical Parameters Reference

$$\text{Rayleigh Range} = z_R = \frac{\pi w_0^2}{\lambda} \approx 3m \tag{C1}$$

$$\text{Diffraction Angle} = \Theta = \arctan\frac{w_0}{z_R} = \arctan\frac{\lambda}{\pi w_0} \approx \frac{w_0}{z_R} \tag{C2}$$

$$\text{q-param} = q(z) = iz_r + z - z_0 = q_0 + z - z_0, q_0 = iz_R \tag{C3}$$

$$\text{Radius of Curvature} = R_c = z - z_0 + \frac{z_R^2}{z - z_0} = D + \frac{z_R^2}{D} \tag{C4}$$

$$R_c \approx \begin{cases} \infty & (D << z_R; \text{Near}) \\ z & (z >> z_R, z_0; \text{Far Field}) \\ 2z_R & (D = z_R; \text{Maximum Curvature}) \end{cases}$$